

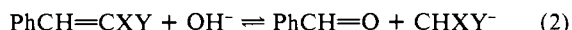
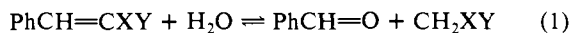
Nucleophilic Addition to Olefins. 13.¹ Kinetics of Hydrolysis of Benzylidene-1,3-indandione

Claude F. Bernasconi,* Alan Laibelman, and Janie L. Zitomer

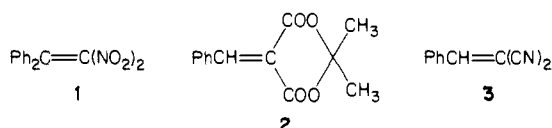
Contribution from the Thimann Laboratories of the University of California, Santa Cruz, California 95064. Received May 2, 1985

Abstract: A complete kinetic analysis of the four-step hydrolysis of benzylidene-1,3-indandione into benzaldehyde and 1,3-indandione in 50% Me₂SO-50% water is reported. The four steps (see Scheme 1) are (1) nucleophilic addition of hydroxide ion or water to form the adduct T_{OH}⁻, (2) carbon protonation of T_{OH}⁻ to form T_{OH}⁰, (3) oxygen deprotonation of T_{OH}⁰ to form T_O⁻, and (4) breakdown of T_O⁻ into benzaldehyde and 1,3-indandione or its anion. There is also a direct water-catalyzed pathway from T_{OH}⁰ to benzaldehyde and 1,3-indandione. Rate and equilibrium constants of the various steps are compared with analogous parameters in the hydrolysis of benzylidenemalononitrile, β-nitrostyrene, benzylidene Meldrum's acid, and 1,1-dinitro-2,2-diphenylethylene. The following conclusions emerge. (1) The equilibrium constants of the carbanion-forming steps (step 1 forward, step 2 reverse, step 4 forward) correlate fairly well with the pK_a values of the corresponding parent carbon acids 1,3-indandione, malononitrile, nitromethane, Meldrum's acid, and 1,1-dinitroethane, although steric as well as other factors make the correlations less than perfect. (2) The *intrinsic* rate constants (*k* for *K* = 1) for the carbanion-forming steps (step 1 with OH⁻, and step 4) decrease with increasing resonance stabilization of the carbanion, just as is the case for the deprotonation of the corresponding parent carbon acids. However, the effect of the activating substituent(s) on the intrinsic rates of these steps is only about half (on a logarithmic scale) as large as for the proton transfer. (3) The effect of the activating substituent(s) on the intrinsic rates of *water* addition to the olefin, and of the direct water-catalyzed breakdown of T_{OH}⁰ to products, is significantly smaller than for step 1 (OH⁻ attack) and *k*₄, and in some cases even reversed, with the intrinsic rate being *higher* for the system with substituents capable of strong resonance. This is attributed to a special transition-state stabilization by internal hydrogen bonding from the water to the oxygen anion in these water-catalyzed reactions.

The hydrolysis of olefins which are activated by electron-withdrawing substituents, and particularly its reverse, the Knoevenagel condensation, are important reactions in organic chemistry. For a benzylidene derivative the overall process can be represented by eq 1 at pH < pK_a^{CH₂XY} and by eq 2 at pH > pK_a^{CH₂XY}.

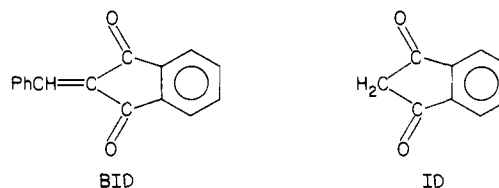


The mechanism is basically the same, irrespective of the identity of X and Y, and is shown in Scheme I. However, the kinetic behavior of a given system depends strongly on how X and Y affect the various steps in the scheme. By carrying out a detailed kinetic analysis of each step we have been able to understand the kinetic behavior of the hydrolysis of a number of compounds such as 1,1-dinitro-2,2-diphenylethylene (1),³ benzylidene Meldrum's acid



(2),⁴ and benzylidenemalononitrile (3).^{2,5} These detailed studies have usually led to significant revisions of earlier mechanistic notions about these reactions.^{4,5}

The present paper reports an analysis of the various steps in the hydrolysis of benzylidene-1,3-indandione (BID) in 50% Me₂SO-50% water (v/v). A major motivation for this work was to be able to estimate the *intrinsic* rate constants (*k* for *K* = 1) for steps 1 and 4 in Scheme I, and to compare them with those obtained for other XY substituents. This is of interest in the context of what factors determine intrinsic barriers in carbanion forming reactions.⁶



Results

General Features. Rates were all determined spectrophotometrically, either in a stopped-flow apparatus or in a conventional spectrophotometer. Runs were conducted both in the forward (hydrolysis) and in the reverse direction (condensation of benzaldehyde with 1,3-indandione (ID)). Under certain conditions (high pH) the OH adduct of BID (T_{OH}⁻) accumulates to detectable levels, and hence a number of experiments were also conducted by letting T_{OH}⁻ react with an acid solution (pH-jump experiments).

In the majority of cases the loss (or increase) of BID was monitored at its λ_{max} 343 nm (ε 19 500). In some experiments changes in the concentration of 1,3-indandione anion (ID⁻), which has a λ_{max} 415 nm (ε 2300), or of T_{OH}⁻ (λ_{max} 430 nm, ε 2200) were monitored. All kinetic runs were conducted under pseudo-first-order conditions, with BID (or in the reverse direction with ID) as the minor component. Standard reaction conditions were 20 °C in 50% Me₂SO-50% water (v/v), at constant ionic strength of 0.5 M maintained with KCl.

pH-Rate Profiles. Overview. Figure 1 shows pH-rate profiles for a variety of processes. The circles refer to *k*_h which is the pseudo-first-order rate constant for disappearance of BID, mostly measured at 343 nm (λ_{max} of BID). Below pH ≈ 8 T_{OH}⁻ does not accumulate to significant levels and thus *k*_h also refers to product formation. In this pH range *k*_h can alternatively be determined via

$$k_h = K_h k_c \quad (3)$$

with *K*_h being the equilibrium constant of hydrolysis (defined for eq 1) and *k*_c being the bimolecular rate constant for condensation of benzaldehyde with ID. The *k*_h values obtained in this manner are shown as filled circles.

(1) Part 12: Bernasconi, C. F.; Kanavarioti, A.; Killion, R. B., Jr. *J. Am. Chem. Soc.* **1985**, *107*, 3612.

(2) Bernasconi, C. F.; Fox, J. P.; Kanavarioti, A.; Panda, M., submitted for publication.

(3) Bernasconi, C. F.; Carre, D. J.; Kanavarioti, A. *J. Am. Chem. Soc.* **1981**, *103*, 4850.

(4) (a) Bernasconi, C. F.; Leonarduzzi, G. D. *J. Am. Chem. Soc.* **1982**, *104*, 5133, 5143. (b) Bernasconi, C. F.; Leonarduzzi, G. D. *Ibid.* **1980**, *102*, 1361.

(5) (a) Bernasconi, C. F.; Howard, K. A.; Kanavarioti, A. *J. Am. Chem. Soc.* **1984**, *106*, 6827. (b) Bernasconi, C. F.; Kanavarioti, A.; Killion, R. B., Jr. *Ibid.* **1985**, *107*, 3612.

(6) For a recent review, see: Bernasconi, C. F. *Pure Appl. Chem.* **1982**, *54*, 2335.

Scheme I

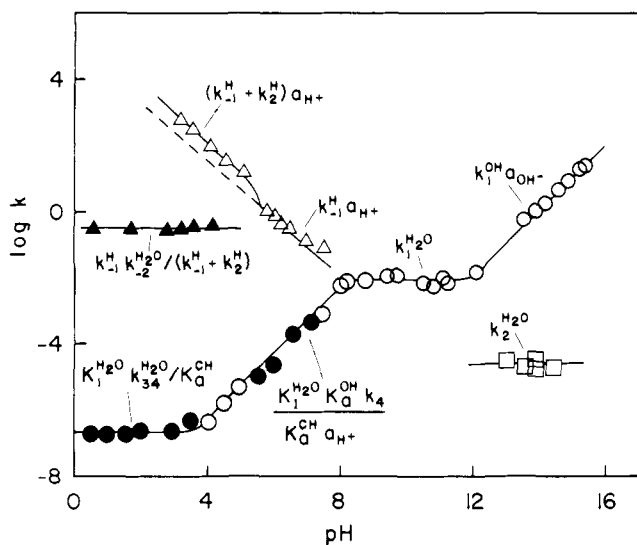
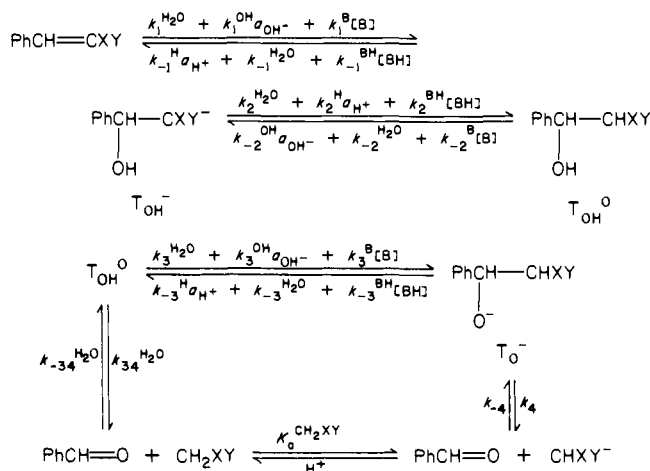


Figure 1. pH-rate profiles: (O) k_h measured in the hydrolysis direction; (●) k_h calculated from k_c measured in the condensation direction; (□) conversion of T_{OH^-} to products by rate-limiting carbon protonation; (Δ) τ_1^{-1} reaction of T_{OH^-} with acid; (▲) τ_2^{-1} reaction of T_{OH^-} with acid.

Above pH 8 T_{OH^-} accumulates to significant concentrations and product formation occurs as a separate, slower reaction (squares in Figure 1).

When a basic solution containing T_{OH^-} is acidified in the stopped-flow apparatus (pH jump), T_{OH^-} is consumed rapidly with pseudo-first-order rate constants indicated as triangles in Figure 1. This process can be monitored either at λ_{max} of T_{OH^-} (decrease) or at λ_{max} of BID (increase). At pH below ≈ 5 an additional kinetic process which is pH-independent appears (filled triangles). It manifests itself as a further increase of BID but is not visible at λ_{max} of T_{OH^-} .

In Figure 1 we have made mechanistic assignments in the various pH ranges using the symbolism of Scheme I. Note that $K_1^{\text{H}_2\text{O}}$ is defined as $k_1^{\text{H}_2\text{O}}/k_{-1}^{\text{H}}$, K_a^{OH} as $K_3^{\text{H}_2\text{O}} = k_3^{\text{H}_2\text{O}}/k_{-3}^{\text{H}}$, and K_a^{CH} as $(K_2^{\text{H}_2\text{O}})^{-1}$ with $K_2^{\text{H}_2\text{O}} = k_2^{\text{H}_2\text{O}}/k_{-2}^{\text{H}}$. In the following sections we describe in some detail how the various processes were measured and how the mechanistic assignments were arrived at. The raw data are in Tables S1–S7 (supplementary material).⁷

Reaction of BID with Hydroxide Ion, pH 13.53–15.24. k_h is proportional to a_{OH^-} in this range. The reaction leads to the formation of T_{OH^-} , with

$$k_h = k_1^{\text{OH}} a_{\text{OH}^-} \quad (4)$$

T_{OH^-} , which is quite stable for several minutes under these con-

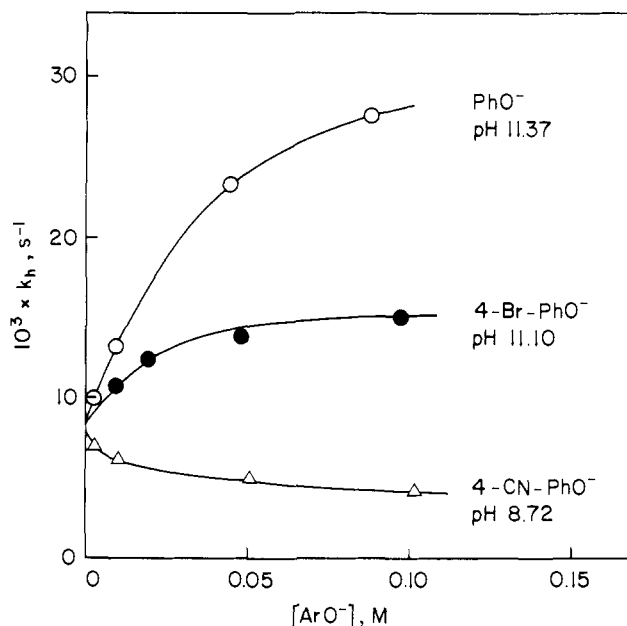


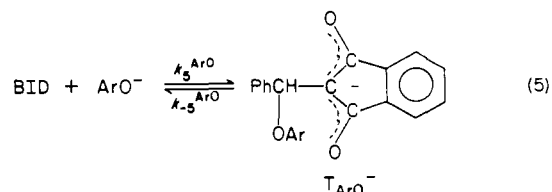
Figure 2. Dependence of k_h for the hydrolysis of BID on aryl oxide ion concentration.

ditions, was identified by its UV/vis spectrum which is very similar to that of ID^- , and by the fact that it is slowly converted to a mixture of benzaldehyde and ID^- .

Reaction of BID with Water, pH 8.00–12.05. In this pH region k_h was measured in phenol and *p*-bromo- and *p*-cyanophenol buffers. k_h is pH independent but shows some dependence on buffer concentration. The data included in Figure 1 are extrapolated to zero buffer concentration.

Figure 2 shows three representative buffer plots. They indicate a complex buffer dependence. With phenoxide there is significant catalysis but a leveling off at high concentrations. With *p*-bromophenoxide the catalysis is much weaker, again with a leveling off. With *p*-cyanophenol there is a slight decrease in k_h with increasing buffer concentration.

These results are consistent with k_h referring to water addition to BID ($k_1^{\text{H}_2\text{O}}$). Buffer catalysis can be attributed to general base catalysis of this reaction ($k_1^{\text{B}[\text{B}]}$) which is a very common finding for water addition to activated olefins^{4a,5a} and to numerous other electrophiles.⁸ The leveling off, and the buffer inhibition in the *p*-cyanophenol buffers, must be a consequence of competing addition of the aryl-oxide ion to BID (eq 5) which acts as a pre-



equilibrium. With phenoxide ion reaction 5 could be studied directly in the stopped-flow apparatus. We obtained $k_5^{\text{ArO}} = 3.93 \times 10^3 \text{ M}^{-1} \text{ s}^{-1}$, $k_{-5}^{\text{ArO}} = 49 \text{ s}^{-1}$, and $K_5^{\text{ArO}} = k_5^{\text{ArO}}/k_{-5}^{\text{ArO}} = 80.1 \text{ M}^{-1}$.

Taking into account general base catalysis and reaction 5 leads to a k_h given by

$$k_h = \frac{k_1^{\text{H}_2\text{O}} + k_1^{\text{B}[\text{ArO}^-]}}{1 + K_5^{\text{ArO}}[\text{ArO}^-]} \quad (6)$$

In the light of eq 6 one can appreciate that with the most basic phenoxide ion catalysis is relatively strong at low concentration because the ratio $k_1^{\text{B}[\text{ArO}^-]}/k_1^{\text{H}_2\text{O}}$ is relatively large and $K_5^{\text{ArO}}[\text{ArO}^-]$ is still $\ll 1$. However, the rate-retarding effect of reaction 5

(7) See paragraph concerning supplementary materials at the end of this paper.

(8) Jencks, W. P. *Acc. Chem. Res.* 1976, 9, 425; 1980, 13, 161.

becomes also quite pronounced at high concentrations because K_5^{ArO} and hence $K_5^{ArO}[ArO^-]$ is relatively large. Incidentally, plots (not shown) of $k_h(1 + K_5^{ArO}[ArO^-])$ vs. $[ArO^-]$ afford excellent straight lines with pH-independent (within experimental error) slopes of $k_1^B = 2.13 \text{ M}^{-1} \text{ s}^{-1}$ (pH 10.68), $2.46 \text{ M}^{-1} \text{ s}^{-1}$ (pH 11.37), and $2.55 \text{ M}^{-1} \text{ s}^{-1}$ (pH 12.05). This shows that eq 6 describes the data very well.

With the less basic aryl oxide ions, both the catalytic and the inhibiting effects become weaker since both $k_1^B/k_1^{H_2O}$ and K_5^{ArO} are reduced.

As can be seen in Figure 1 the scatter in the $k_h = k_1^{H_2O}$ values is somewhat worse than in most other pH ranges. We attribute this to some problems in obtaining good first-order kinetic plots under our standard reaction conditions ($[BID]_0 \approx 2 \times 10^{-5} \text{ M}$). Better linearity of the first-order plots could be achieved by using very small initial BID concentrations ($<10^{-5} \text{ M}$) which, however, was at the expense of an optimal signal-to-noise ratio.

Similar behavior has been observed in the hydrolysis of benzylidenemalononitrile^{5a} which could be attributed to the reaction of malononitrile anion (formed as a product) with remaining benzylidenemalononitrile. In the present case it cannot be the reaction of ID^- with remaining BID because ID^- is formed much more slowly (see $k_2^{H_2O}$ in Figure 1). A more likely candidate is the reaction of T_{OH}^- with BID; this interpretation would be consistent with the observation that first-order behavior is restored when low $[BID]_0$ is used, and also when the reaction is conducted at high pH since here the hydroxide ion concentration is orders of magnitude larger than the T_{OH}^- concentration and competes much more effectively for BID.

Hydrolysis of BID and Condensation of PhCHO with ID, pH 0.53–8.14. Hydrolysis rates were determined in cacodylate, acetate, and methoxyacetate buffers (open circles in Figure 1).

Condensation rates were measured in the same buffer, and also in HCl solutions. In one set of experiments ID was treated with a large excess of benzaldehyde at pH 4.98 (acetate buffer), and k_c for the condensation reaction was determined from eq 7 by

$$k_{obsd} = k_h + k_c[PhCHO]_0 \quad (7)$$

measuring k_{obsd} at six different $[PhCHO]_0$, covering a range from 6.67×10^{-3} to $9.87 \times 10^{-2} \text{ M}$. In conjunction with k_h determined from hydrolysis at the same pH, this afforded $K_h = 2.51 \times 10^{-4} \text{ M}$.

The thus determined K_h was then used to calculate k_h (filled circles in Figure 1) at different pH values by either one of two methods. In the first, k_c was obtained from k_{obsd} determined at four to five $[PhCHO]_0$ via eq 7 as described above, and k_h was calculated from eq 3. In the second k_{obsd} was measured at single benzaldehyde concentrations and k_h evaluated according to

$$k_h = \frac{k_{obsd}K_h}{K_h + [PhCHO]_0} \quad (8)$$

Most of our data at very low pH were obtained by measuring condensation rates. This was much more convenient because the hydrolysis is very slow (half-lives of $\approx 4 \times 10^6 \text{ s}$ or 10^3 h).

A test for buffer catalysis proved negative; no enhancement of k_h in a cacodylate buffer (seven concentrations from 0.004 to 0.20 M) at pH 6.95 could be detected. This shows that the k_4 step must be rate limiting in the pH-dependent range between pH 4 and 8, with k_h being given by

$$k_h = K_1^{H_2O}K_2^{H_2O}K_3^{H_2O}k_4/a_{H^+} = K_1^{H_2O}K_a^{OH}k_4/K_a^{CH}a_{H^+} \quad (9)$$

Other possibilities which show the same pH dependence for k_h are rate-limiting carbon protonation of T_{OH}^- by water ($k_h = K_1^{H_2O}k_2^{H_2O}/a_{H^+}$), or rate-limiting oxygen deprotonation by OH^- ($k_h = (K_1^{H_2O}k_3^{OH}/K_a^{CH})\alpha_{OH^-}$). Both of these alternatives are excluded by the absence of buffer catalysis.

The plateau below pH 4 is due to the direct conversion of T_{OH}^0 into benzaldehyde and ID, with k_h given by

$$k_h = (K_1^{H_2O}/K_a^{CH})k_{34}^{H_2O} \quad (10)$$

An alternative interpretation which would be consistent with the

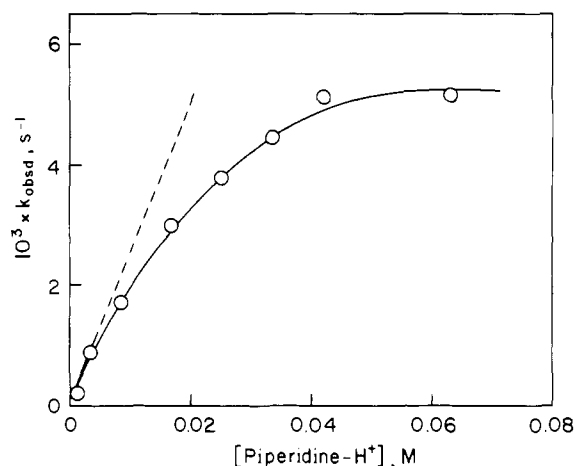


Figure 3. Dependence of k_{obsd} for the conversion of T_{OH}^- to products on piperidinium ion concentration.

pH independence of k_h is rate-limiting carbon protonation of T_{OH}^- by H_3O^+ ($k_h = K_1^{H_2O}k_2^H$). This alternative can be excluded on the basis of the low numerical value of k_h ; with $K_1^{H_2O} = 1.62 \times 10^{-8} \text{ M}$ and $k_2^H = 3.62 \times 10^5 \text{ M}^{-1} \text{ s}^{-1}$ (see below), we have $K_1^{H_2O}k_2^H = 5.86 \times 10^{-3} \text{ s}^{-1}$ which is 3.90×10^4 fold larger than the observed $k_h = 1.5 \times 10^{-7} \text{ s}^{-1}$.

Conversion of T_{OH}^- into PhCHO and ID^- , pH 11.50–13.94. This reaction was studied in KOH solution, and in phenol and piperidine buffers. Because of the similarity in λ_{max} and ϵ_{max} of T_{OH}^- and ID^- , the reaction was monitored at 390 nm where the $\Delta\epsilon$ is relatively large ($\epsilon_{ID^-} - \epsilon_{T_{OH}^-} = 1750 - 1180 = 570$).

The buffer experiments were conducted by first generating T_{OH}^- in a KOH solution in the absence of buffer. This procedure circumvents the problem of competing formation of the piperidine⁹ or phenoxide ion adduct (eq 5) of BID. It is only after T_{OH}^- was completely formed that the buffer was added and conversion to PhCHO and ID^- was monitored.

k_{obsd} was observed to be independent of pH but subject to strong general acid catalysis. With the phenol buffer k_{obsd} increases linearly with $[PhOH]$ (plot not shown) while with piperidine buffer there is a leveling off at high concentration as shown in Figure 3. These results are consistent with rate-limiting carbon protonation of T_{OH}^- by water and by general acids; i.e., k_{obsd} is given by

$$k_{obsd} = k_2^{H_2O} + k_2^{BH}[BH] \quad (11)$$

at low $[BH]$. The leveling off at high $[BH]$ in the piperidine buffer indicates a change from rate-limiting proton transfer to rate rate-limiting k_4 ($k_{obsd} = K_a^{OH}k_4/K_a^{CH} = 5.14 \times 10^{-3} \text{ s}^{-1}$). This change comes about because at low buffer concentration we have $k_{-2}^B[B] \ll K_a^{OH}k_4/a_{H^+}$, while at high buffer concentrations $k_{-2}^B[B] \gg K_a^{OH}k_4/a_{H^+}$.

It should be noted that a pH-independent rate with general acid catalysis could, in principle, also be consistent with rate-limiting oxygen deprotonation of T_{OH}^0 by OH^- and by general bases; i.e.,

$$k_{obsd} = \frac{a_{H^+}}{K_a^{CH}}(k_3^{OH}a_{OH^-} + k_3^B[B]) = \frac{K_w}{K_a^{CH}}k_3^{OH} + \frac{K_a^{BH}}{K_a^{CH}}k_3^B[BH] \quad (12)$$

with K_a^{BH} being the acid dissociation constant of BH. However, with $pK_w = 15.9$, $pK_a^{CH} = 5.87$ (see below), and $k_{obsd} = 2.5 \times 10^{-5} \text{ s}^{-1}$ (at $[BH] = 0$), one would calculate $k_3^{OH} = 2.7 \times 10^5 \text{ M}^{-1} \text{ s}^{-1}$, almost four orders of magnitude lower than k_3^{OH} typically observed in similar reactions.^{3,4} Hence eq 12 can be safely excluded.

The reaction was also measured in the condensation direction in KOH solution at pH 13.94, with benzaldehyde as the excess

(9) Bernasconi, C. F.; Stronach, M. W., unpublished results.

component. The results were treated according to

$$k_{\text{obsd}} = k_2^{\text{H}_2\text{O}} + (k_2^{\text{OH}}K_w/K_a^{\text{OH}}K_4)[\text{PhCH=O}]_0 \quad (13)$$

From the dependence on $[\text{PhCH=O}]_0$ one obtains $k_2^{\text{OH}}K_w/K_a^{\text{OH}}K_4 = 2.52 \times 10^{-3} \text{ M}^{-1} \text{ s}^{-1}$. In conjunction with K_a^{OH} and K_4 determined below, this affords a value for k_2^{OH} .

Reaction of T_{OH^-} with Acid (pH Jumps), pH 0.6 to 7.5. We shall identify the pseudo-first-order rate constants referring to the open triangles in Figure 1 as τ_1^{-1} , the ones referring to the filled triangles as τ_2^{-1} . τ_1^{-1} is associated with a decrease in T_{OH^-} and an increase in BID and is visible over the entire pH range. It shows a very small buffer dependence (5 to 10% increase at 0.1 M buffer concentration) at $\text{pH} \geq 5.8$ but strong general acid catalysis at $\text{pH} 5.1$ (e.g., three- to fivefold increase in rate at $[\text{BH}] \approx 0.03 \text{ M}$). Between $\text{pH} 5.1$ and 5.8 there is a transition on the pH-rate profile in which the line for τ_1^{-1} is displaced upward by approximately 0.5 log unit. At the same time the ΔOD observed at λ_{max} of BID, but not that observed at λ_{max} of T_{OH^-} , decreases by about 40%.

τ_2^{-1} is associated with an increase in BID which corresponds to the missing $\sim 40\%$ in the ΔOD for τ_1^{-1} , but it is not visible at λ_{max} of T_{OH^-} . It only appears below $\text{pH} 5$ with τ_2^{-1} being pH independent but showing general base catalysis.

These observations can be interpreted as follows. At $\text{pH} \geq 5.8$, τ_1^{-1} refers to acid-catalyzed breakdown of T_{OH^-} to BID and hence is given by

$$\tau_1^{-1} = k_{-1}^{\text{H}}a_{\text{H}^+} + k_{-1}^{\text{BH}}[\text{BH}] \approx k_{-1}a_{\text{H}^+} \quad (14)$$

with $k_{-1}^{\text{BH}}[\text{BH}]$ being very small for $[\text{BH}] \leq 0.1 \text{ M}$. In more strongly acidic solution, i.e., at $\text{pH} < \text{p}K_a^{\text{CH}}$, carbon protonation of T_{OH^-} becomes competitive with the k_{-1}^{H} process and thus

$$\tau_1^{-1} = (k_{-1}^{\text{H}} + k_2^{\text{H}})a_{\text{H}^+} + k_2^{\text{BH}}[\text{BH}] \quad (15)$$

Since carbon protonation by buffer acids is usually very effective, the $k_2^{\text{BH}}[\text{BH}]$ term in eq 15 is quite large,¹⁰ as observed.

The τ_2^{-1} process is the final equilibration which involves conversion of T_{OH^0} (formed during the τ_1^{-1} process) into BID. This conversion proceeds via T_{OH^-} which now is a steady-state intermediate. Thus τ_2^{-1} is given by

$$\tau_2^{-1} = \frac{(k_{-2}^{\text{H}_2\text{O}} + k_2^{\text{B}}[\text{B}])k_{-1}^{\text{H}}a_{\text{H}^+}}{(k_{-1}^{\text{H}} + k_2^{\text{H}})a_{\text{H}^+} + k_2^{\text{BH}}[\text{BH}]} \quad (16)$$

At zero buffer concentration eq 16 simplifies to

$$\tau_2^{-1} = k_2^{\text{H}_2\text{O}}k_{-1}^{\text{H}}/(k_2^{\text{H}} + k_{-1}^{\text{H}}) \quad (17)$$

which is consistent with the observed pH independence (filled triangles in Figure 1).

Dissection of Rate and Equilibrium Constants. All rate and equilibrium constants obtained in this study are summarized in Tables I and II. Since for most constants the method by which they were obtained is obvious from the discussion of the previous sections, only the less trivial cases are discussed here.

$k_{-1}^{\text{H}_2\text{O}}$ was obtained from k_1^{OH} and $K_1^{\text{OH}} = K_1^{\text{H}_2\text{O}}/K_w$, while k_2^{H} was calculated as the difference in the slopes according to eq 15 and 14. Equation 17 could then be solved for $k_2^{\text{H}_2\text{O}}$. Combining this latter value with k_2^{H} yields $K_a^{\text{CH}} = k_2^{\text{H}_2\text{O}}/k_2^{\text{H}}$, and by combining K_a^{CH} , K_w , and $k_2^{\text{H}_2\text{O}}$, one obtains k_2^{OH} .

$\text{p}K_a^{\text{OH}}$ was estimated at 14.7. This estimate is based on the assumption that $\text{p}K_a^{\text{OH}}$ is slightly higher than the $\text{p}K_a^{\text{OH}}$ of T_{OH^0} derived from benzylidene Meldrum's acid. This $\text{p}K_a^{\text{OH}}$ is ≈ 12.8 in aqueous solution.^{5a} The increase brought about by a change from water to 50% Me_2SO is estimated at 1.5 to 1.7 pK units¹¹ which would bring the $\text{p}K_a^{\text{OH}}$ of the benzylidene Meldrum's acid adduct to ≈ 14.3 – 14.5 .

K_4 was found from the overall equilibrium constant which, at $\text{pH} \ll \text{p}K_a^{\text{ID}}$, is given by

$$K_h = K_1^{\text{H}_2\text{O}}K_a^{\text{OH}}K_4/K_a^{\text{CH}} \quad (18)$$

Table I. Hydrolysis of BID. Rate and Equilibrium Constants for the Steps in Scheme I in 50% Me_2SO –50% Water (v/v) at 20 °C^a

constant	value
Step 1	
$K_1^{\text{H}_2\text{O}}$ ($\text{p}K_1^{\text{H}_2\text{O}}$), M	1.62×10^{-8} (7.79)
$K_1^{\text{OH}} = K_1^{\text{H}_2\text{O}}/K_w$, M ⁻¹	1.29×10^8
$k_1^{\text{H}_2\text{O}}$, s ⁻¹	8.90×10^{-3}
k_{-1}^{H} , M ⁻¹ s ⁻¹	5.48×10^5
k_1^{OH} , M ⁻¹ s ⁻¹	1.01×10^2
$k_{-2}^{\text{H}_2\text{O}}$, s ⁻¹	7.83×10^{-7}
k_1^{PhO} , M ⁻¹ s ⁻¹	2.39 ^d
k_{-1}^{PhOH} , M ⁻¹ s ⁻¹	4.66×10^{-4}
Step 2	
$(K_2^{\text{H}_2\text{O}})^{-1} = K_a^{\text{CH}}$ ($\text{p}K_a^{\text{CH}}$), M	1.35×10^{-6} (5.87) ^e
$k_2^{\text{H}_2\text{O}}$, s ⁻¹	2.48×10^{-5}
k_{-2}^{OH} , M ⁻¹ s ⁻¹	2.78×10^5
k_2^{H} , M ⁻¹ s ⁻¹	3.62×10^5
$k_{-2}^{\text{H}_2\text{O}}$, s ⁻¹	0.49
Step 3	
$K_3^{\text{OH}} = K_a^{\text{OH}}$ ($\text{p}K_a^{\text{OH}}$)	$\approx 2.0 \times 10^{-15}$ (14.7)
Step 34	
$K_{34}^{\text{H}_2\text{O}}$, M	2.09×10^{-2}
$k_{34}^{\text{H}_2\text{O}}$, s ⁻¹	1.45×10^{-5}
$k_{-34}^{\text{H}_2\text{O}}$, s ⁻¹	6.94×10^{-4}
Step 4	
K_4 , M	4.58×10^6
k_4 , s ⁻¹	3.22×10^6
k_{-4} , M ⁻¹ s ⁻¹	0.703
Reaction 5 ^f	
K_5^{PhO}	80.2
k_5^{PhO}	3.93×10^3
k_{-5}^{PhO}	49

^a $K_h = 2.51 \times 10^4 \text{ M}$ is the equilibrium constant for $\text{BID} + \text{H}_2\text{O} \rightleftharpoons \text{PhCHO} + \text{ID}$. ^b $\text{p}K_w = 15.90$. ^c Phenoxide ion catalyzed water addition or phenol catalyzed loss of OH^- from T_{OH^-} . ^d Average from three pH values. ^e This compares with $\text{p}K_a^{\text{ID}} = 6.35$. ^f With $\text{ArO}^- = \text{PhO}^-$.

Table II. Proton Transfer Rate Constants (Step 2 in Scheme I) Involving Buffers

BH	$\text{p}K_a^{\text{BH}}$	k_2^{BH} , M ⁻¹ s ⁻¹	k_{-2}^{B} , M ⁻¹ s ⁻¹
Cl_2CHCOOH	2.15	1.71×10^5	3.26
ClCH_2COOH	3.71	3.91×10^3	2.71×10^4
AcOH	5.78	3.72×10^2	3.02×10^2
piperidine-H ⁺	11.02	2.75×10^{-1}	3.88×10^4
PhOH	11.47	1.15×10^{-1}	4.58×10^4

Incidentally with K_4 and K_a^{OH} now available, k_2^{OH} can also be found from eq 13. The value of k_2^{OH} obtained from eq 13 ($1.83 \times 10^5 \text{ M}^{-1} \text{ s}^{-1}$) is in good agreement with $k_2^{\text{OH}} = 2.78 \times 10^5 \text{ M}^{-1} \text{ s}^{-1}$ determined in the manner described above.

k_2^{B} for chloroacetate and dichloroacetate ion were obtained from initial slopes according to eq 16 (with $k_2^{\text{BH}}[\text{BH}] \ll (k_{-1}^{\text{H}} + k_2^{\text{H}})a_{\text{H}^+}$).

For k_4 there are two sources. One is from data on k_h between $\text{pH} 4$ and 8 (eq 9) which yields $k_4 = 2.97 \times 10^6 \text{ s}^{-1}$; the other is from the plateau of Figure 3 ($k_{\text{obsd}} = K_a^{\text{OH}}k_4/K_a^{\text{CH}}$) which yields $k_4 = 3.47 \times 10^6 \text{ s}^{-1}$, in very good agreement with the first value. We shall adopt the average as the value for k_4 .

Discussion

Our kinetic analysis of the hydrolysis of BID has permitted a determination of most of the rate constants (and hence also of the equilibrium constants) shown in Scheme I. They are summarized in Tables I and II. The only parameters not amenable to direct measurement were the rate constants of step 3, the $\text{p}K_a^{\text{OH}}$ of T_{OH^0} , and k_4 . However, $\text{p}K_a^{\text{OH}}$ was relatively easily estimated and with this estimate the value of k_4 was then also obtained.

It is instructive to compare our results with those obtained for the hydrolysis of similar olefins such as 1,1-dinitro-2,2-diphenylethylene (1),³ benzylidene Meldrum's acid (2),⁴ benzylidenemalononitrile (3),⁵ and 3,4-methylenedioxy- β -nitrostyrene

(10) See, e.g.: Kresge, A. *J. Chem. Soc. Rev.* **1973**, 2, 475.

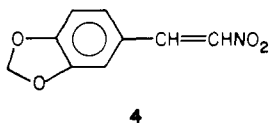
(11) Crowell, T. K.; Kim, T.-R. *J. Am. Chem. Soc.* **1973**, 95, 6781.

Table III. Selected Rate and Equilibrium Constants in the Hydrolysis of Olefins

parameter	3 PhCH=C(CN) ₂		4	BID ^d	1	2
	H ₂ O ^a	50% Me ₂ SO ^b	ArCH=CHNO ₂ ^c H ₂ O		Ph ₂ C=C(NO ₂) ₂ ^e 50% Me ₂ SO	PhCH=C(COO) ₂ C(CH ₃) ₂ ^f H ₂ O
pK _a ^{CH₂XY}	11.39	10.21	10.20	6.35	5.00	4.83
K ₁ ^{H₂O} , M	2.0 × 10 ⁻¹¹	≈ 3.0 × 10 ⁻¹⁰	5.0 × 10 ⁻⁹	1.62 × 10 ⁻⁸	8.1 × 10 ⁻⁷	3.75 × 10 ⁻⁶
pK _a ^{H₂O}	10.7	9.5	8.3	7.79	6.09	5.43
k ₁ ^{H₂O} , s ⁻¹	2.45 × 10 ⁻⁴	1.05 × 10 ⁻³	8.18 × 10 ⁻⁶	8.90 × 10 ⁻³	1.05 × 10 ⁻⁴	0.55
k ₁ ^{OH⁻} , M ⁻¹ s ⁻¹	2.75 × 10 ²	1.00 × 10 ³	0.30	1.01 × 10 ²	12.2	7.45 × 10 ²
pK _a ^{CH⁺}	≈ 8.7	≈ 7.7	8.78	5.87	5.53	2.95
K ₃₄ ^{H₂O} , M	≈ 3.30 × 10 ⁻¹	6.90 × 10 ⁻²		2.09 × 10 ⁻²		
k ₃₄ ^{H₂O} , s ⁻¹	≈ 1.30 × 10 ⁻⁶	≈ 1.05 × 10 ⁻⁶		1.45 × 10 ⁻⁵		
K ₄ , M	≈ 2.74 × 10 ⁻¹	≈ 4.3 × 10 ¹	≈ 3.16 × 10 ³	4.58 × 10 ⁶	very high	very high
pK ₄	0.56	-1.63	-3.50	-6.66		
k ₄	≈ 4.66 × 10 ⁴	≈ 5.9 × 10 ⁵	≈ 6.33 × 10 ²	3.22 × 10 ⁶	> 2 × 10 ⁹	≈ 5 × 10 ⁶

^a 25 °C, ref 5a. ^b 20 °C, ref 5b. ^c Ar = 3,4-methylenedioxyphenyl, 25 °C, ref 11 and 5a. ^d 20 °C, this work. ^e 20 °C, ref 3. ^f 25 °C, ref 4. ^g Refers to C-H acidity of T_{OH}⁰.

(4).¹¹ Table III summarizes selected parameters for the different systems.



Before making detailed comparisons of the various kinetic and thermodynamic parameters among these systems, it is worth pointing out that in all systems except for 3 T_{OH}⁻ accumulates to detectable levels in basic solution. A necessary but insufficient condition for T_{OH}⁻ to become directly observable is that the equilibrium of step 1 can be pushed toward the right at high pH so that $K_1^{H_2O}/a_{H^+} = K_1^{OH^-}a_{OH^-} \gg 1$. Inspection of Table III reveals that even though 3 has the smallest $K_1^{H_2O}$ value it is still large enough for the above condition to be met at pH > 10.7 in water, and at pH > 9.5 in 50% Me₂SO-50% water.

The reason why T_{OH}⁻ is not observable for 3 is that the intermediate is kinetically unstable; i.e., the rate of its conversion to products is faster than the rate of its formation, as discussed in more detail elsewhere.⁵ In solvents of higher Me₂SO content this conversion to products can, however, be slowed down enough as to make T_{OH}⁻ detectable.²

Equilibrium Constants. The various systems summarized in Table II are arranged according to decreasing pK_a^{CH₂XY}. We note that pK₁^{H₂O}, pK_a^{CH}, and pK₄ follow the same rank order as pK_a^{CH₂XY} with one exception (pK_a^{CH} for 4 is larger than pK_a^{CH} for 3). This parallelism is not surprising since each of these equilibrium constants refers to the formation of a RCXY⁻-type carbanion.

In a quantitative sense the correlations of these various pK values with pK_a^{CH₂XY} are by no means perfect, though, as seen in Figures 4-6. In each of these figures we have drawn, somewhat arbitrarily, a straight line of unit slope through the point for 3 in aqueous solution.

There are several factors which lead to the observed deviations from the straight line (note that a positive deviation means the equilibrium is disfavored compared to system 3, a negative deviation that it is favored).

In the K₄ equilibrium (Figure 6) release of steric strain in T₀⁻ derived from BID is likely to be an important factor in enhancing K₄. In systems 1 and 2 (not included in Figure 6), the overall hydrolysis is not measurably reversible, indicating very high K₄ values which must be the consequence of even larger steric effects in these more crowded systems (particularly 1). On the other hand, the large enhancement of K₄ in system 4 is somewhat surprising since the steric effect is expected to be smaller here. One factor which favors K₄ in this system is the increased push by the electron-donating phenyl substituent, but this cannot be the whole explanation. This point will be taken up again when discussing pK₁^{H₂O}.

Enhanced push by the more basic anionic oxygen of T₀⁻ is the principal reason for the enhanced K₄ for 3 in 50% Me₂SO compared to 3 in water.^{5b} Part of the enhancement of K₄ in the BID

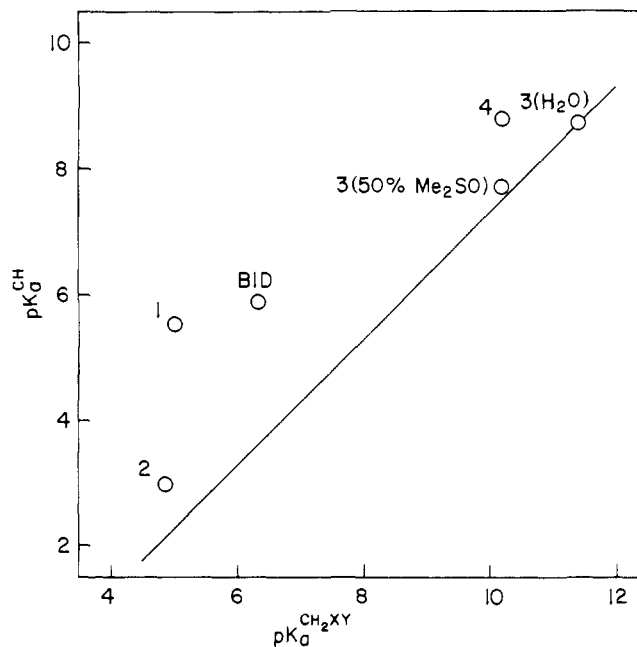


Figure 4. Correlation of pK_a^{CH} (C-H acidity of T_{OH}⁰) with pK_a^{CH₂XY}.

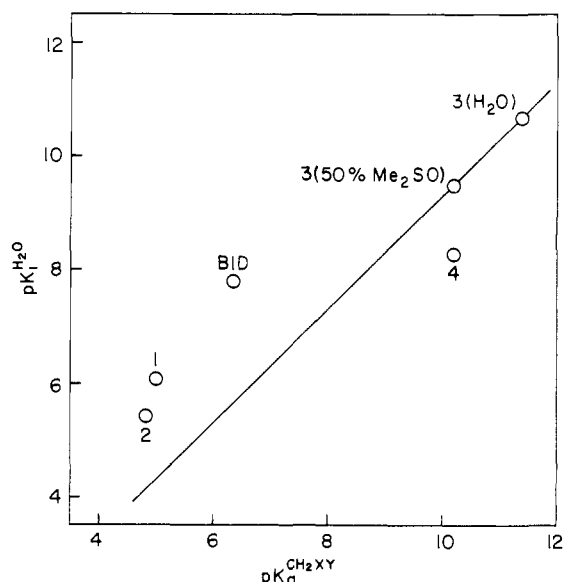


Figure 5. Correlation of pK₁^{H₂O} (water addition to the olefin) with pK_a^{CH₂XY}.

system can also be attributed to this factor since water is used as the reference solvent in drawing the straight line of unit slope.

The correlations of pK_a^{CH} (Figure 4) and pK₁^{H₂O} (Figure 5) with pK_a^{CH₂XY} are very similar to each other, at least with respect

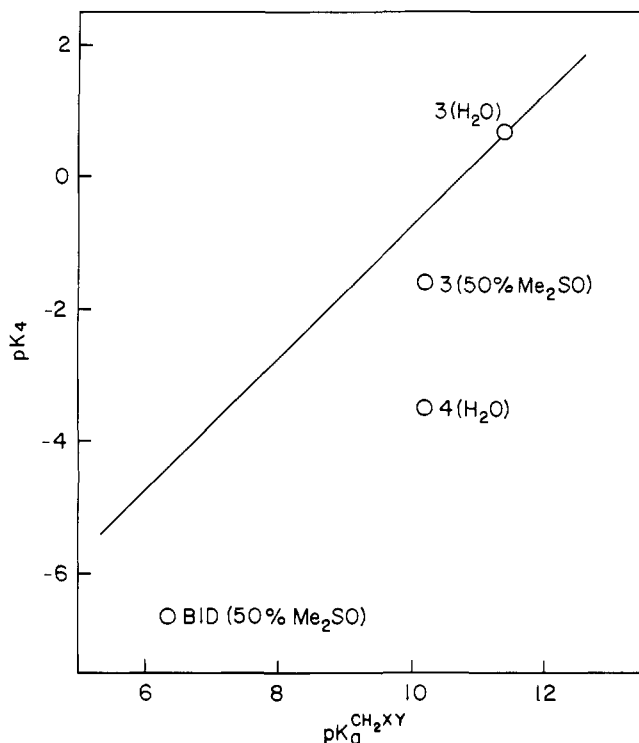


Figure 6. Correlation of pK_4 (breakdown of T_0^- into benzaldehyde and $CHXY^-$) with $pK_a^{CH_2XY}$.

to **1**, **2**, **3**, and BID. They indicate a relatively smaller stability of T_{OH}^- for **1**, **2**, and BID than for **3**, regardless of whether T_{OH}^- is formed by carbon deprotonation of T_{OH}^0 (pK_a^{CH}) or by nucleophilic addition to the olefin ($pK_1^{H_2O}$). One important factor is undoubtedly steric hindrance to coplanarity of the CXY^- moiety, which makes resonance stabilization less effective than in the parent $HCHY^-$.

A second contributing factor has to do with the diminishing polar effect of the $PhCHOH$ (or Ph_2COH) moiety. This polar effect is electron withdrawing as can be seen by the fact that the pK_a^{CH} values are generally lower than the respective $pK_a^{CH_2XY}$ value, despite the less effective resonance effect noted above. (Only for system **1** is the steric hindrance of the resonance so pronounced that $pK_a^{CH} > pK_a^{CH_2XY}$.) This polar effect should affect pK_a^{CH} and $pK_1^{H_2O}$ the most in systems where the resonance effect is not very strong (**3**), and will decrease in importance for more strongly resonance stabilized carbanions. This then has the effect of lowering $pK_1^{H_2O}$ and pK_a^{CH} for **3** much more than for the other systems.

It is noteworthy that **2** deviates less from the line than BID for both pK_a^{CH} and $pK_1^{H_2O}$. This must reflect the fact that the exceptionally high stability of the Meldrum's acid anion is not so much related to strong resonance stabilization but rather to its bislactone-type structure.¹² There is also evidence that intramolecular hydrogen bonding between the OH group and one of the carbonyl oxygens may contribute to the high stability of T_{OH}^- .^{4a}

The positive deviation for **4** on the pK_a^{CH} plot can be explained along similar lines as for the other positively deviating points. The steric effect is probably less important here but the reduction in the polar effect is likely to be more important than in any other system. This is because the resonance effect is largest and also because the $ArCHOH$ group is less electron withdrawing than $PhCHOH$, owing to the electron-donating substituent in the aryl group.

The negative deviation for **4** from the $pK_1^{H_2O}$ plot, showing unusually high reactivity of **4** toward nucleophilic attack, is more

Table IV. Intrinsic Rate Constants Relative to $PhCH=C(CN)_2$ as Reference, $\log(k_0^{(CN)_2}/k_0^{XY})$

	2 PhCH=C- (COO) ₂ C- (CH ₃) ₂	1 Ph ₂ C=C- (NO ₂) ₂ 50% Me ₂ SO	4 ArCH=C- CHNO ₂ H ₂ O
k_1^{OH}	1.86	(2.20) ^b	(3.63) ^b
k_4	(1.78) ^b		(3.96) ^b
$k_1^{H_2O}$	-0.06	(-0.71) ^b	(2.72) ^b
$k_{34}^{H_2O}$	-1.40		2.71
k_p^a	3.9	3.4	5.5
			7.3

^a Refers to proton transfer $CH_2XY + B^- \rightleftharpoons CHXY^- + BH$. Data from ref 22 (ID). Eigen, M.; Ilgenfritz, G.; Kruse, W. *Chem. Ber.* **1965**, *98*, 1623 (Meldrum's acid). Bernasconi, C. F.; Kanavarioti, A. *J. Org. Chem.* **1979**, *44*, 4829 ($CH_2CH(NO_2)_2$). Bernasconi, C. F.; Yu, E., unpublished results (CH_3NO_2). Reference 18 ($RCH(CN)_2$).
^b Values in parentheses are less certain because of relatively long extrapolations required; see text.

difficult to explain. It may be related to the strongly enhanced K_4 which could only partly be accounted for by release of steric strain and increased push by the aryl substituent. As noted before,^{5a} these results indicate a weakening of the C-C bond in **4** compared to the other olefins, and of the C-C bond in T_0^- derived from **4**. The reasons for this weakening remain unclear, though.

Rate Constants, Intrinsic Rates. Inspection of Table III reveals that there is no obvious correlation between rate and equilibrium constants from one system to another. For example, for k_1^{OH} we have **3** (50% Me₂SO) > **2** > BID >> **1** >> **4** which is different from the sequence **2** > **1** > BID > **4** > **3** for $k_1^{H_2O}$.

This lack of correlation is caused by the large differences in the intrinsic barriers,¹³ or intrinsic rates,¹³ between the various systems.

We have attempted to separate the effects on the rate constants which arise from differences in the equilibrium constants, and those which come from differences in the intrinsic barrier, in the following way. Substrate **3** in water was chosen as reference substrate for the reactions in water, substrate **3** in 50% Me₂SO as reference for the reactions in 50% Me₂SO. The rate constants for the other systems were then adjusted in such a way as to make the equilibrium constants the same as for **3**.

For example, $K_1^{H_2O}$ for BID is 54-fold higher than that for **3** in the same solvent. If $K_1^{H_2O}$ were as low as that for **3**, this decrease would have to come about by a combination of a lower $k_1^{H_2O}$ with a higher k_{-1}^H for BID. We shall assume that the reduction in $k_1^{H_2O}$ and the increase in k_{-1}^H contribute equally to the change in the equilibrium constant, i.e., the "Brønsted slope", $d \log k_1^{H_2O} / d \log K_1^{H_2O} = -d \log k_{-1}^H / d \log K_1^{H_2O} = 0.5$. Thus the adjusted $k_1^{H_2O}$ value for BID, $(k_1^{H_2O})_{adj}^{ID}$, is $8.90 \times 10^{-3} \times (54)^{-1/2} = 1.21 \times 10^{-3} s^{-1}$; the adjusted k_{-1}^H , $(k_{-1}^H)_{adj}^{ID}$, value is $5.49 \times 10^5 (54)^{1/2} = 4.03 \times 10^6 M^{-1} s^{-1}$.

We can now regard the ratios $(k_1^{H_2O}(CN)_2)/(k_1^{H_2O}(CN)_2)_{adj}^{ID} = (k_{-1}^H)^{(CN)_2}/(k_{-1}^H)_{adj}^{ID}$ as an approximation of the ratio of the intrinsic rate constants, $k_0^{(CN)_2}/k_0^{ID}$, for water addition to the double bond of **3** vs. BID.

Approximate ratios of intrinsic rate constants for the other steps, and for the comparison of **3** with the other olefins, were obtained in a similar manner, always assuming $d \log k_{forward} / d \log K_{forward} = -d \log k_{reverse} / d \log K_{forward} = 0.5$. They are summarized in Table IV, along with similar ratios for the deprotonation of CH_2XY by amines or carboxylate ions.

In discussing these ratios we have to keep their approximate nature in mind. In cases where the equilibrium constants for a given step are quite similar to that in the reference system, relatively little adjustment was needed. In these cases the errors which are introduced by the possibly erroneous assumption that $d \log k_{forward} / d \log K_{forward}$ is always 0.5 will have a minor effect, and our $k_0^{(CN)_2}/k_0^{XY}$ ratios are likely to represent a good approximation. In the cases where a large adjustment was required,

(12) (a) Arnett, E. M.; Maroldo, S. G.; Schilling, S. L.; Harrelson, J. A. *J. Am. Chem. Soc.* **1984**, *106*, 6759. (b) Huisgen, R.; Ott, H. *Tetrahedron* **1959**, *6*, 253.

(13) The intrinsic barrier, ΔG_0^\ddagger , is defined as ΔG^\ddagger when $\Delta G^\circ = 0$; the intrinsic rate, k_0 , as k when $K = 1$ ($\Delta G^\circ = 0$).

the uncertainty in the estimated $k_0^{(\text{CN})_2}/k_0^{\text{XY}}$ ratio is much larger. These latter cases are identified by parentheses in Table IV.

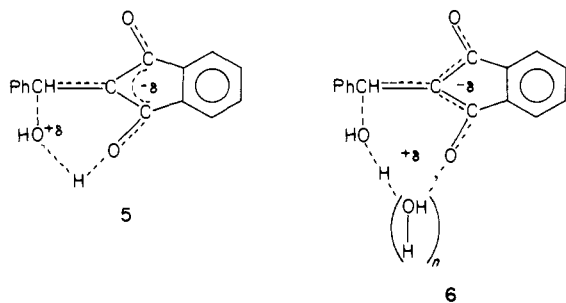
With these reservations in mind we note the following patterns: (1) OH^- addition to the double bond (k_1^{OH}) and the breakdown of T_0^- into CHXY^- and the respective aldehyde (k_4) follow the same qualitative pattern as the proton transfers (k_p); i.e., $k_0^{(\text{CN})_2}/k_0^{\text{XY}}$ increases or k_0^{XY} decreases with increased resonance stabilization of the carbanion. This kind of pattern has been noted before,^{5a,6,14,15} but it is significant that our new results with the BID system fit in very nicely with the previously obtained results.

(2) The $k_0^{(\text{CN})_2}/k_0^{\text{XY}}$ ratios for the k_1^{OH} and the k_4 process are remarkably similar to each other and both roughly half (on a log scale) the corresponding ratios for proton transfer. The larger ratios for the proton transfers have been attributed to the diminishing capability of the carbanionic carbon to act as a good hydrogen bond acceptor,^{6,16-19} a factor which cannot play a role in the other reactions.

In our work with amine nucleophiles we noted that the $k_0^{(\text{CN})_2}/k_0^{\text{XY}}$ ratios for addition to olefinic double bonds were even smaller than the ones now observed for the k_1^{OH} and k_4 processes.^{6,14} This led us to suggest that when a reaction involves no change in hybridization of the CXY carbon (as in the addition to olefins) k_0 is less sensitive to the nature of XY than when a change in hybridization is involved (as in the proton transfer and the k_4 process). The present results seem to indicate now that the sensitivity of k_0 to XY may be just about the same for the OH^- addition as it is for the k_4 process; i.e., differences in hybridization seem to play a minor role.

(3) The $k_0^{(\text{CN})_2}/k_0^{\text{XY}}$ ratios for water addition ($k_1^{\text{H}_2\text{O}}$) show a markedly different dependence on XY than the ones observed for k_1^{OH} and k_4 . With the two nitro compounds $\log(k_0^{(\text{CN})_2}/k_0^{\text{XY}})$ is strongly positive as expected although the magnitude of these ratios is significantly less than for the k_1^{OH} process. However, with BID, and particularly with the Meldrum's acid derivative, $\log(k_0^{(\text{CN})_2}/k_0^{\text{XY}})$ is *negative*, indicating that the intrinsic rate constants are *larger* for the formation of the *more strongly* resonance-stabilized carbanions!

These comparisons suggest that BID and **2** behave abnormally with respect to the $k_1^{\text{H}_2\text{O}}$ process. A plausible reason for this enhanced reactivity toward water addition but not toward OH^- addition is that the transition state derives extra stabilization from intramolecular hydrogen bonding solvation, as shown in **5** or **6** for the BID system.



This kind of internal solvation, which probably plays only a minor role in system **3**, provides stabilization both for the developing positive and negative charge. The stabilization of the negative charge could well be the major effect, though. According to our current understanding, a principal reason why intrinsic rates for the formation of resonance-stabilized carbanions are depressed is that hydrogen bonding solvation (by the solvent) of the developing negative charge at the periphery of XY (oxygen atoms in nitro or carbonyl compounds) is retarded in the transition state.²¹

(14) Bernasconi, C. F.; Murray, C. J.; Fox, J. P., Carré, D. J. *J. Am. Chem. Soc.* **1983**, *105*, 4349.

(15) Bernasconi, C. F.; Murray, C. F. *J. Am. Chem. Soc.* **1984**, *106*, 3257.

(16) Eigen, M. *Angew. Chem., Int. Ed. Engl.* **1964**, *3*, 1.

(17) Bell, R. P. "The Proton in Chemistry", 1st ed.; Cornell University Press: Ithaca, N.Y., 1959; p 155.

(18) Hibbert, F. *Compr. Chem. Kinet.* **1977**, *8*, 97.

(19) Ritchie, C. D. *J. Am. Chem. Soc.* **1969**, *91*, 6749.

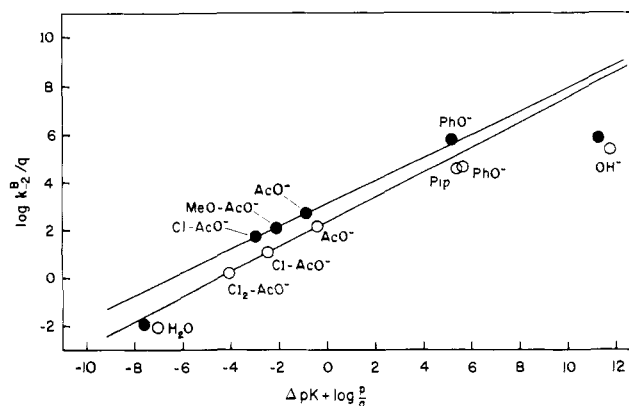
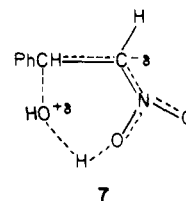


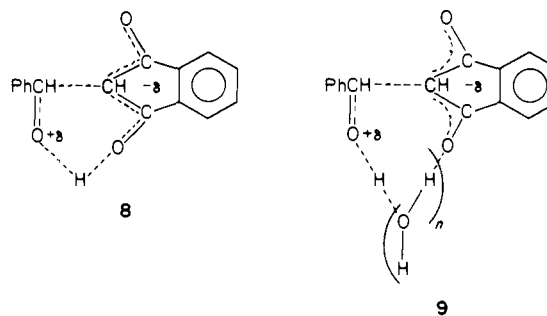
Figure 7. Eigen plots for the carbon deprotonation of T_{OH}^0 derived from BID (open circles) and the deprotonation of ID (filled circles).

This lag in solvation appears to be due, in part, to an unfavorable entropy factor associated with the immobilization of the solvent. The internal solvation shown in **5** or **6** would not be as unfavorable entropically and thus the free energy of the transition would be correspondingly lowered.

As noted above, even though the $\log(k_0^{(\text{CN})_2}/k_0^{\text{XY}})$ values for **1** and **4** seem more "normal", they are 1.1 and 1.5 log units, respectively, lower than for OH^- addition. This could indicate that for the nitro compounds, too, there is some transition state stabilization by internal solvation, as, e.g., in **7**.



(4) For the $k_{34}^{\text{H}_2\text{O}}$ step we note a similar, even more pronounced inversion of the $k_0^{(\text{CN})_2}/k_0^{\text{XY}}$ ratio (negative log value) as for the $k_1^{\text{H}_2\text{O}}$ step in the BID system. We attribute this again to a transition-state stabilization by internal solvation as shown in **8** or **9**.



Proton Transfers. Our investigation has yielded a number of rate constants for proton transfer at carbon of the T_{OH}^- adduct. They are summarized in Table II while Figure 7 shows an Eigen¹⁶ plot for the deprotonation of T_{OH}^0 along with a similar plot for the deprotonation of ID.²²

The Brønsted $\beta = 0.52$ defined by the carboxylate ions is quite similar to $\beta = 0.48$ for the deprotonation of ID,²² but the Brønsted line for T_{OH}^0 is approximately 0.8 log unit (at $\Delta pK + \log(p/q) = 0$) lower than that for ID. This displacement of the Brønsted line undoubtedly reflects a steric effect.

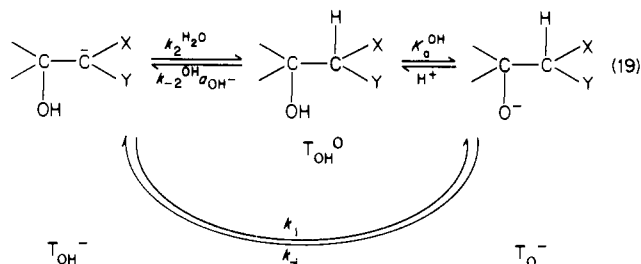
The points for water and hydroxide ion show their typical¹⁰ negative deviations from the Brønsted line. It is noteworthy that the carbon deprotonation of T_{OH}^0 by hydroxide ion does not show any special acceleration compared to the deprotonation of ID by

(20) Bernasconi, C. F.; Fornarini, S. *J. Am. Chem. Soc.* **1980**, *102*, 2810.

(21) Bernasconi, C. F. *J. Am. Chem. Soc.*, in press.

(22) Bernasconi, C. F.; Paschalis, P. *J. Am. Chem. Soc.*, in press.

the same base. This indicates that the competing k_i - k_{-i} pathway (eq 19), which involves an intramolecular proton switch,²³ plays a minor, if any, role in the BID system.



This is consistent with the behavior of **1** and **2**. However, it contrasts with our findings for **3**^{2,5b} where the k_i - k_{-i} pathway contributes significantly to the reaction; i.e., $k_2^{H_2O}$ has to be replaced by $k_2^{H_2O} + k_i$ and k_{-2}^{OH} by $k_{-2}^{OH} + K_a^{OH}k_{-i}/K_w$, with k_i and $K_a^{OH}k_{-i}/K_w$ being actually the dominant terms. The reasons why the intramolecular proton switch is a significant pathway in some systems but not in others have been discussed elsewhere.²⁴

Experimental Section

Materials. 1,3-Indandione (Aldrich) was recrystallized from 100% ethanol, mp 130–131 °C (lit. 130 °C²⁵) prior to use. Benzylidene-1,3-indandione (BID) was prepared from benzaldehyde and 1,3-indandione in ethanol, with piperidine as catalyst, according to the procedure of Behera and Nayak,²⁶ mp 152 °C (lit. 152–153 °C²⁷). Benzaldehyde was

(23) Such an intramolecular proton switch most likely involves a water bridge in the transition state.²⁴

(24) Bernasconi, C. F.; Hibdon, S. A.; McMurry, S. E. *J. Am. Chem. Soc.* **1982**, *104*, 3459.

(25) Sieglitz, G. *Chem. Ber.* **1951**, *84*, 607.

purified by washing, drying, and vacuum distillation, according to the method of Perrin.²⁸

Phenols were recrystallized from hexane prior to use. Chloroacetic acid was recrystallized from petroleum ether. Methoxyacetic acid was distilled, and piperidine was distilled following refluxing over CaH₂. All other reagents were commercial products used without further purification.

Kinetics. The fast reactions were monitored on a Durrum stopped-flow apparatus with computerized data handling.²⁹ For OH⁻ and PhO⁻ addition, KOH or buffered PhOH solutions were mixed with solutions of BID containing a little HCl (to prevent hydrolysis in the reservoir syringe).

The slow reactions were measured in a Perkin-Elmer Model 559A spectrophotometer. In most cases, cuvettes containing buffer solution were equilibrated at 20 °C, and either BID or ID, followed (after a few minutes) by benzaldehyde, was added by injecting a few microliters of concentrated stock solution. For the slow conversion of T_{OH}⁻ to products the usual method was the same as above, but a higher concentration of BID (5×10^{-4} M) was required in order to achieve high enough OD changes.

pH's were measured as described previously.⁵

Acknowledgment. This research was supported by Grant CHE-8315374 from the National Science Foundation.

Registry No. BID, 5381-33-9; ID, 606-23-5; PhCHO, 100-52-7.

Supplementary Material Available: Kinetic data, Tables S1–S10 (9 pages). Ordering information is given on any current masthead page.

(26) Behera, R. K.; Nayak, A. *Indian J. Chem.* **1976**, *14B*, 223.

(27) Pritchard, R. B.; Lough, C. E.; Currie, D. J.; Holmes, H. L. *Can. J. Chem.* **1968**, *46*, 775.

(28) Perrin, D. D.; Armarego, W. L. F.; Perrin, D. R. "Purification of Laboratory Chemicals", 2nd ed.; Pergamon Press: New York, 1980; p 553.

(29) Software developed by Dr. F. A. Brand.

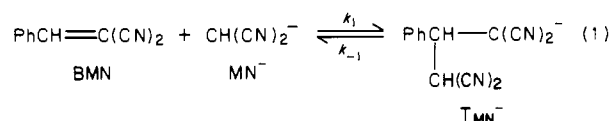
Nucleophilic Addition to Olefins.¹ 14. Kinetics of the Reaction of 1,3-Indandione Anion with Benzylidene-1,3-indandione

Claude F. Bernasconi,* Alan Laibelman, and Janie L. Zitomer

Contribution from the Thimann Laboratories of the University of California, Santa Cruz, California 95064. Received May 2, 1985

Abstract: The rate and equilibrium constants of the reversible addition of 1,3-indandione anion (ID⁻) to benzylidene-1,3-indandione (BID) have been determined in 50% Me₂SO–50% water at 20 °C: $k_1 = 7.23 \times 10^3 \text{ M}^{-1} \text{ s}^{-1}$, $k_{-1} = 9.35 \times 10^{-3} \text{ s}^{-1}$, $K_1 = 7.73 \times 10^5 \text{ M}^{-1}$. The *intrinsic* rate constant for this reaction is about 300-fold lower than for the analogous reaction of malononitrile anion (MN⁻) with benzylidenemalononitrile (BMN). This is consistent with numerous previous observations according to which reactions involving more strongly resonance-stabilized carbanions have lower intrinsic rates (higher intrinsic barriers). The ratio of 300 in the intrinsic rate constants is larger than the corresponding ratios in the addition of hydroxide ion to BMN vs. BID, or the addition of MN⁻ vs. ID⁻ to benzaldehyde. This is not surprising since the reactions of ID⁻ with BID and the one of MN⁻ with BMN both involve *two* carbanionic sites. Our results, as well as similar findings in the comparison of the MN⁻/BMN system with the nitromethane anion/ β -nitrostyrene system, constitute Marcus-type behavior, although the *quantitative* adherence to a modified Marcus equation is not very good. The pK_a values of both the keto and the enol form of the BID/ID⁻ adduct and proton-transfer rates involving the keto form were determined. The enol content of the adduct is much higher than that of ID itself. This is attributed to intramolecular hydrogen bonding in the adduct. Proton transfer at carbon of the adduct is, for a given ΔpK , slower by a factor of ~ 12 than at carbon of ID, showing the operation of a steric effect.

We recently reported a kinetic study of the Michael addition of malononitrile anion (MN⁻) to benzylidenemalononitrile (BMN) in water and in 50% Me₂SO–50% water.² In this latter solvent, the reaction has an equilibrium constant, $K_1 = k_1/k_{-1}$, of 1.45



$\times 10^5 \text{ M}^{-1}$ and is quite rapid, with $k_1 = 9.50 \times 10^5 \text{ M}^{-1} \text{ s}^{-1}$ and $k_{-1} = 6.52 \text{ s}^{-1}$.

The high rate constants are not surprising in the context of other reactions which lead to the formation or destruction of malono-

(1) Part 13: Bernasconi, C. F.; Laibelman, A.; Zitomer, J. L. *J. Am. Chem. Soc.*, preceding paper in this issue.

(2) Bernasconi, C. F.; Zitomer, J. L.; Fox, J. P.; Howard, K. A. *J. Org. Chem.* **1984**, *49*, 482.